Hindawi
Scanning
Volume 2020, Article ID 5642124, 8 pages
https://doi.org/10.1155/2020/5642124

Research Article

A Cost-Effective Method for Preparing Robust and Conductive Superhydrophobic Coatings Based on Asphalt

Wenbin Li,[1,2] **Yong Wang**,[1,2] **Yanting Feng**,[1,2] **Qing Wang**,[1,2] **Xuexia Xu**,[1,2] **Guowei Li**,[1,2] **Guozhen Dong**,[1,2] **Shangqian Jing**,[1,2] **Ersong Chen**,[1] **Xiaoliang Fan**,[3] **and Peng Wang**[3]

[1]*State Grid Hebei Electric Power Research Institute, Shijiazhuang 050021, China*
[2]*State Grid Hebei Energy Technology Service Co., Ltd., Shijiazhuang 050021, China*
[3]*School of Energy, Power and Mechanical Engineering, North China Electric Power University, Baoding 071003, China*

Correspondence should be addressed to Wenbin Li; wenbinli1975@126.com and Peng Wang; wang.peng.ncepu@foxmail.com

Received 20 April 2020; Accepted 4 December 2020; Published 24 December 2020

Academic Editor: Guosong Wu

The wide application of superhydrophobic materials is mainly hindered by the poor mechanical robustness and complicated preparation method. To overcome these problems, we tried to make a combination of hierarchical and self-similar structure by the means of a simple spraying method. By adding nanofiller (carbon nanotube) and microfiller (graphite powder and expanded graphite), the hierarchical structure was constructed. By further doping the fillers in the commercial asphalt uniformly, the self-similar structure was prepared. Based on the aforementioned work, the as-prepared sample could withstand the sandpaper abrasion for 12.00 m under 4.90 kPa. Moreover, this superhydrophobic coating demonstrated good conductivity, superior self-cleaning property, and excellent corrosion resistance. The integration of conductivity with the superhydrophobicity might open new avenues for ground grid applications.

1. Introduction

The steel is widely used in our daily life and industry due to its relatively low price, excellent mechanical strength, and superior machinability [1–3]. However, most steel is prone to be corroded, which results in massive economic losses. Many methods have been developed to prohibit the corrosion [4–7]. Particularly, superhydrophobic materials, which can be fabricated by the combination of micro/nanostructure and low surface energy, are attracting more and more attention because the water droplets can maintain nearly spherical shape on them and roll off easily [8–11]. Based on this extreme repellency, many researches have tried to use the superhydrophobic materials to protect corrosion [12–14]. For instance, Cao et al. fabricated a superhydrophobic film which could protect the metal substrate for a long time [15]. Zhang et al. prepared a superhydrophobic coating by combining the epoxy resin with carbon nanotubes, which can effectively protect the Q235 carbon steel [16].

However, the Achilles' heel for superhydrophobic surfaces is the poor mechanical durability. Most superhydrophobic surfaces are prone to be damaged by a slight scratch, or even finger contact [17, 18]. To overcome this weakness, three different methods were developed. First, Lu et al. introduced a "Paint+Adhesive" method which tried bonding the hydrophobic particles using the adhesives [19]. Second, Verho et al. adapted hierarchical structure which tried to utilize the relatively robust microstructure to protect the fragile nanostructure [20]. Third, the self-similar structure is also a potential method which let the new exposed part maintain superhydrophobicity because they are similar in texture and functionality with the abrade parts [21].

The electrical conductivity is also a key consideration because it is crucial in many practical applications. For instance, Q235 steel is widely used as ground grid in the electricity substation due to its cheap price and relatively low electrical resistance. Then, the excellent electrical conductivity should be guaranteed when we tried to use superhydrophobic

coating to protect the ground grid [22]. To achieve superhydrophobicity and excellent conductivity simultaneously, scattering carbon-based fillers in the polymer matrix is the main solution. For instance, Hejazi et al. fabricated hair-like superhydrophobic carbon nanotube structure using a template method, which achieved superhydrophobicity without any modification [23]. Gu et al. prepared superhydrophobic surface by coating polystyrene onto the carbon nanotube membrane [24]. Wang et al. constructed a superhydrophobic coating by mixing the graphene with the polydimethylsiloxane [25]. Nevertheless, the aforementioned conductive/superhydrophobic materials have the weakness of mechanical robustness.

In our previous work, a superhydrophobic/conductive material based on the mixture of epoxy and carbon nanotubes has been prepared [26]. The asphalt is widely used in our daily life as the pavement due to its outstanding mechanical strength [27]. Compared with the epoxy, the asphalt has many different specialties, which lead to some special applications such as the pavement. Here, we tried to use the asphalt as the basement to enhance the mechanical strength. In order to obtain self-similar structure, the conductive fillers were uniformly dispersed in the asphalt matrix. In order to further obtain hierarchical structure, both microscale filler (graphite powder and expanded graphite) and nanoscale filler (multiwall carbon nanotube) were utilized. Thus, the hierarchical and self-similar structures were combined which endowed the superhydrophobic coating with outstanding conductivity, excellent mechanical robustness, and superior self-cleaning performance. Moreover, this superhydrophobic coating was achieved by simply spraying, which has the potential for large-scale production.

2. Materials and Methods

2.1. Materials. The 10# asphalt, 70# asphalt, Q235 steel plate, and expanded graphite (EG) were purchased from a local market. The multiwalled carbon nanotubes with a mean diameter and length of 9.5 nm and 1.5 μm were purchased from Nanocyl Co. Ltd., Belgium (NC7000). 1*H*,1*H*,2*H*,2*H*-per-fluorooctyltriethoxysilane ($C_8F_{13}H_4Si(OCH_2CH_3)_3$, FAS) were purchased from Aladdin Reagent Co., Ltd., Shanghai, China. All other chemicals were bought from Sinopharm Chemical Reagent Co., Ltd. (SCRC, China) and used as received.

2.2. The Pretreatment of the Q235 Plate. The Q235 steel plates with dimensions of 20 mm × 20 mm × 1.5 mm were utilized as the substrates. Before using, the Q235 substrates were abraded to be the 800# sandpaper and then ultrasonically cleaned in deionized water.

2.3. Preparation of the Superhydrophobic Coating. The schematic of the fabrication process can be found in Figure 1. First, 1.6 g 10# asphalt and 0.4 g 70 # asphalt were mixed into 7.0 g tetrahydrofuran (THF) by mechanical stirring for 4 h, which was marked as solution A. Separately, 0.6 g graphite powder, 0.15 g MWCNTs, 0.03 g EG, and 0.2 g FAS were sequentially dissolved into 8 g THF by means of mechanical

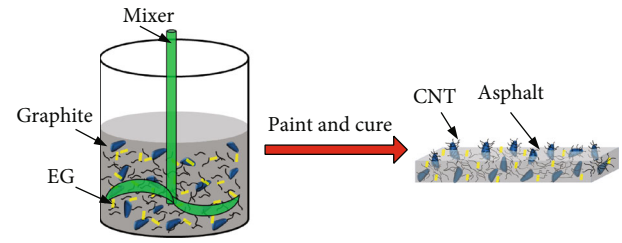

Figure 1: The schematic of the fabrication process.

stirring, which was defined as solution B. It should be noted that we further altered the amount of MWCNTs and EG for the purpose of improving the electrical conductivity. Then, the solution A was mixed with solution B. After stirring for 4 h, the mixture A was obtained. In the next step, the mixture A was sprayed onto the Q235 steel with the help of spray gun under the pressure of 0.4 MPa. Finally, the coating was cured at room temperature for 24 h. The thickness of the as-prepared coating was ~0.45 mm.

2.4. Characterization. The surface microstructures of the superhydrophobic coating were investigated by a scanning electron microscope (SEM, TESCAN Vega3), and the element compositions were assessed from the equipped energy-dispersive spectroscopy (EDS). Before the SEM test, a thin Au film (~2-3 nm) was sputtered onto the samples. The true color confocal microscope was employed to measure the surface roughness. The water contact angles (CAs) were evaluated by a home-made contact angle meter. A high-speed camera (Revealer 2F04) was utilized to assess the sliding angles (SAs). The 5 μL water droplets were adapted in the aforementioned CA and SA tests.

For the resistivity test, the coating was sprayed on a glass slide (76 mm × 26 mm × 2 mm). A DC bridge (QJ84, Shanghai Zhengyang Instrument Factory, China) was utilized to investigate the volume resistivity according to Chinese standard GB/T 2439-2001. The volume resistivity (ρ) was calculated as follows:

$$\rho = R \times \frac{S}{L}, \tag{1}$$

where R is the electrical resistance of the coating, S is the cross-sectional area, and L is the length of the coating. The conductivity (s) is the reciprocal of the volume resistivity.

The CHI760E electrochemical workstation (Shanghai CH Instruments) was utilized to investigate the polarization curves. We used the three-electrode system and set the scanning rate at 1 mV/s. The specimen and a platinum electrode were adapted as the working and counter electrode, respectively. A saturated calomel electrode (SCE) was employed as the reference electrode.

2.5. The Abrasion Test. In the abrasion test, the superhydrophobic coating was faced down to the rough surface of 200# SiC sandpaper. Then, a weight of 200 g (4.90 kPa) was put on the top of the Q235 substrate. With the help of

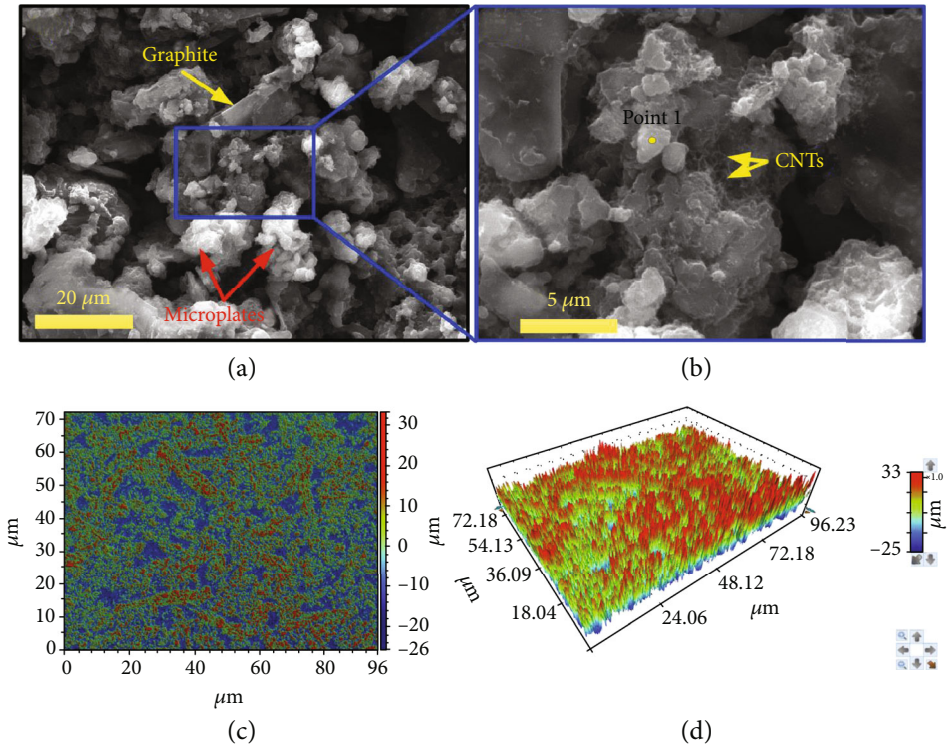

FIGURE 2: The SEM image of the as-prepared superhydrophobic sample with (a) low and (b) high magnification. (c) 2D and (d) 3D true color confocal microscope images of the as-prepared sample.

external force, the specimen was dragged along the ruler for 20 cm, which was defined as one abrasion cycle.

3. Results and Discussion

In this study, the hierarchical structure was prepared by means of adding both microscale filler and nanoscale filler. The SEM observation confirmed the existence of the hierarchical structure. Many microscale bulges (2-20 μm) could be found from Figure 2(a), which came from the EG and graphite. We further amplified the magnification of SEM observation. Then, many MWCNTs could be found which were on and between the microbulges (Figure 2(b)). We further utilized the true color confocal microscope to evaluate the surface morphology (Figures 2(c) and 2(d)). The surface roughness was calculated to be ~6.55 μm, indicating the microscale roughness of the as-prepared superhydrophobic sample.

To detect the chemical composition, the EDS measurement was carried out at the area of Figure 2(b). The C, O, F, and Si components could be detected from Figure 3(a). We attributed the F component to the FAS, which played a vital role in the low surface energy. The Au component came from the Au sputtering prior to the SEM observation. Therefore, this coating obtained superhydrophobicity by means of the combination of hierarchical structure and the low surface energy. It can be found that eight spherical shape water droplets were randomly scattered on the surface (Figure 3(b)), indicating the outstanding superhydrophobicity. We further calculated the CAs and SAs to quantitatively evaluate the wetting state, and this coating exhibited a high CA of 163° and a low SA of 5°. Thus, it is reasonable to deduce that this coating demonstrated stable Cassie-Baxter state where the water droplets were suspended on the surface [28, 29].

XPS measurement was performed to further investigate the surface chemical composition of the as-prepared superhydrophobic surface. Figure 4 shows the survey spectra of the sample. It can be found that the Si 2p, Si 2s, C 1s, O 1s, and F 1s peaks are detected from the surface. Figure 4(b) shows curve-fitted F 1s core-level spectra of the sample. A dominant peak appearing at 689.32 eV corresponds to fluorine bonded as CF_x in the FAS chain indicating that F is present in same bonding environment as that of FAS [30]. A shoulder peak at higher binding energy of 689.75 eV could be associated with Si-F_x interaction [31]. This confirms the presence of fluoride groups on the silica particles [32]. Curve-fitted Si 2p core-level spectra of the sample are showed in Figure 4(c). Si 2p core-level spectra show a dominant peak at 104.15 eV, which corresponds to -Si-OH or Si-F_x species. Low-intense component peak around 102.64 eV could be due to SiO_2-based network. Figure 4(d) shows the multielement spectra of C 1s; observed peaks at 284.50, 284.78, 285.60, 292.00, and 294.27 eV are ascribed to C-Si, C-C, C-O, CF_2, and CF_3, respectively [30–32].

The universal utilization of superhydrophobic materials is hindered by their poor robustness. In other words, the micro/nanostructures which are indispensable for constructing the superhydrophobicity are destructed easily. To solve this problem, the asphalt was utilized as the binder which is widely used in pavement for its excellent mechanical strength

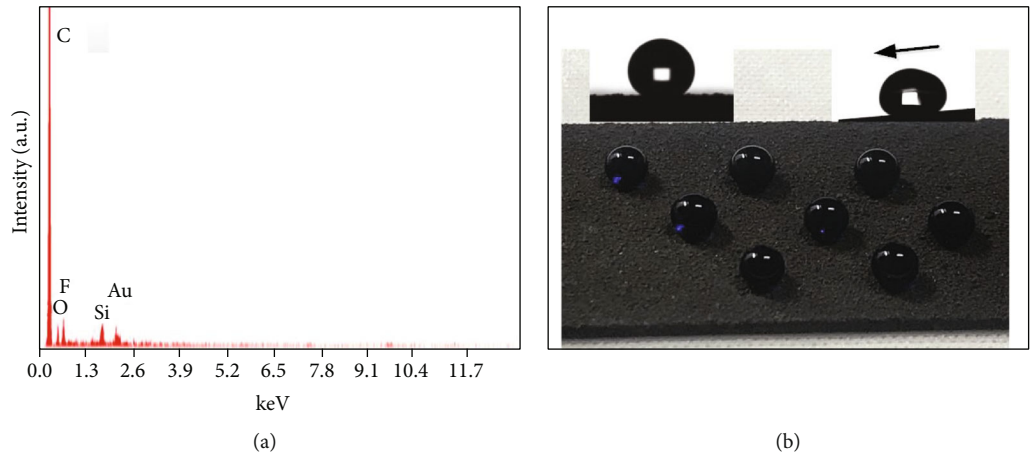

Figure 3: (a) EDS test of point 1 in Figure 2(b). (b) Photograph of water drops deposited on the superhydrophobic sample.

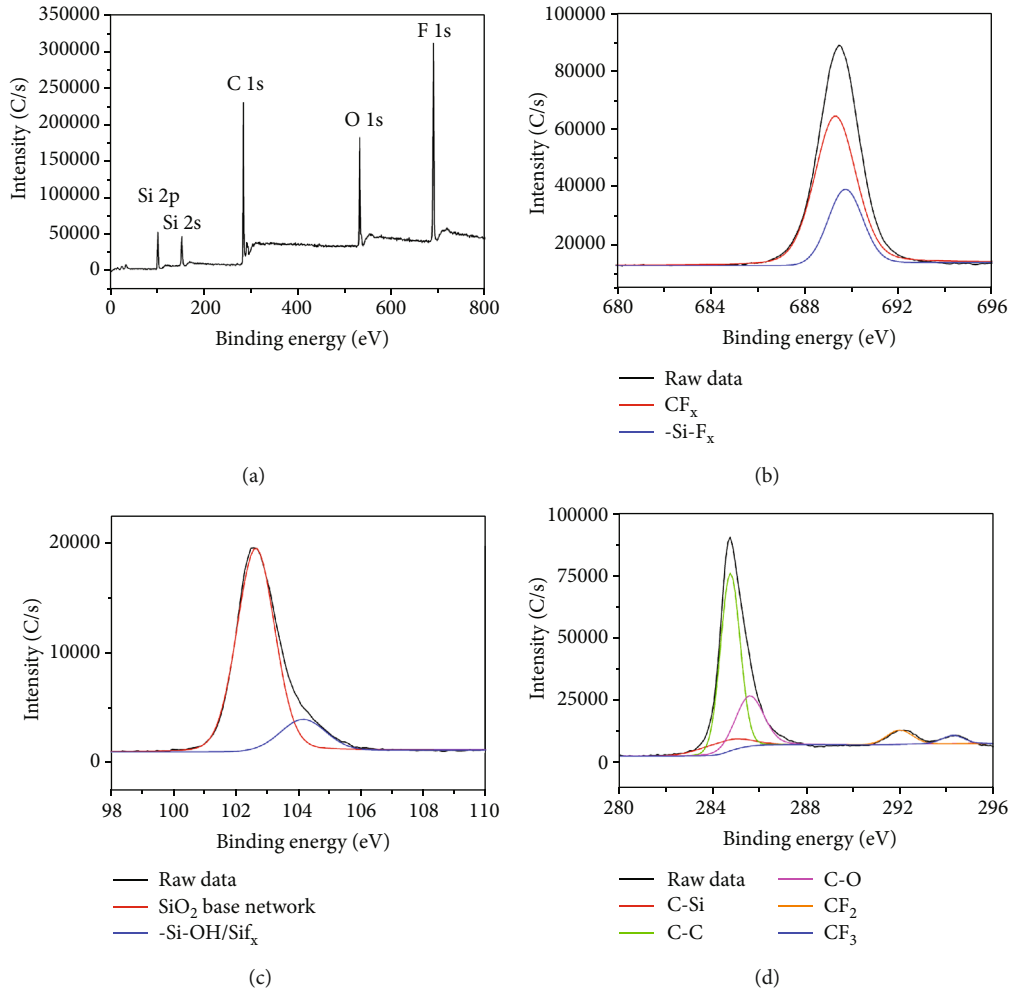

Figure 4: XPS measurement of the graphene superhydrophobic composite. (a) Survey XPS spectrum of the as-prepared superhydrophobic surface. (b) F 1s, (c) Si 2p, and (d) C 1s XPS spectrum of the sample.

and bonding force. At the same time, both micro- and nanofillers were doped in the asphalt matrix to guarantee the formation of hierarchical structure which would enhance the mechanical durability. The sandpaper abrasion test has been widely utilized to evaluate the mechanical robustness [33–41]. Tian et al. further pointed out that the abrasion distance and applied pressure are two key factors to facilitate comparison among different researches [42].

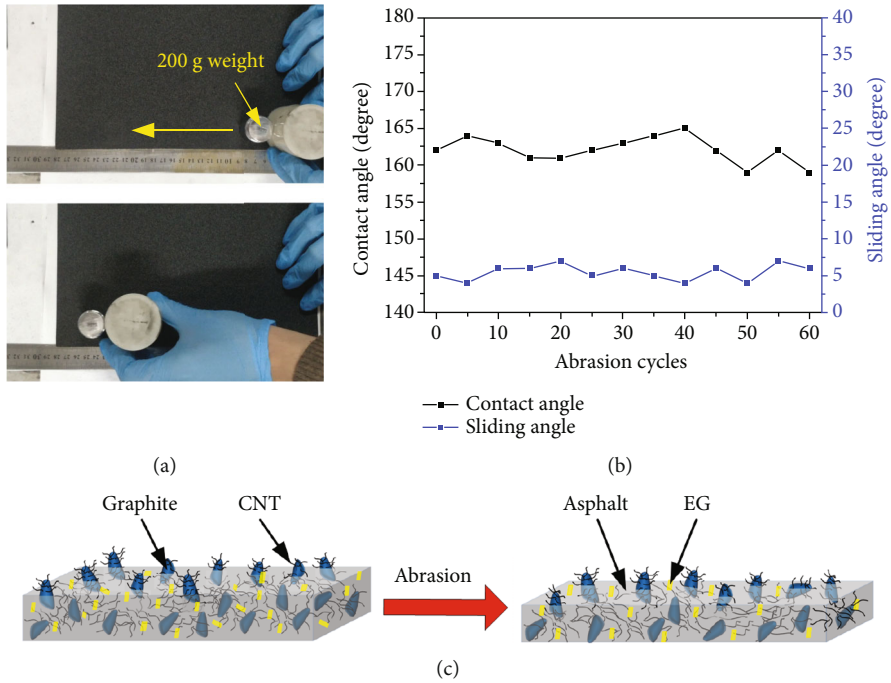

Figure 5: (a) Images of the processes and results of destruction by sandpaper abrasion. (b) The CAs and SAs on the as-prepared sample as a function of abrasion cycle. (c) The schematic of antiabrasion mechanism.

Thus, the sandpaper abrasion test was performed in this research. First, the sample was faced down to the rough surface of SiC sandpaper (200#). Then, a weight of 200 g (4.90 kPa) was put on the top of the sample, as shown in Figure 5(a) and Movie S1. By applying the external force, the sample moved along the ruler for 20 cm as one abrasion cycle. Although some powders could be found during the abrasion process, the superhydrophobicity was retained by watching the behavior of dropping waters. The quantitative changes in CAs and SAs during the abrasion process could be further found in Figure 5(b). Even after 60 abrasion cycles, the CA was 159° and the SA was 6°, indicating the outstanding mechanical robustness. Meanwhile, it was found that the thickness of the coating reduced from ~0.45 mm to ~0.10 mm. We ascribe the retention of superhydrophobicity to the self-similar structure (Figure 5(c)), which makes the undamaged layer of the superhydrophobic coating similar to the exposed parts in functionality and texture.

The conductivity of the materials has received more and more attention recently. On the one hand, the conductive coating could shed off the accumulated electrons and then improve the reliability of the microelectronic device. On the other hand, the excellent conductivity is indispensable for some special application such as the ground grid. In this research, we tried to optimize the electrical property by means of altering the amount of the MWCNTs and EGs. The electrical conductivity and antiabrasion ability were investigated simultaneously, and the results are summarized in Table 1. The detailed test method of the electrical conductivity and antiabrasion ability can be found in the experiment section. With the addition of conductive fillers, the electrical conductivity is increased, but the antiabrasion property decreased simultaneously. Thus, how to make a balance between the electrical conductivity and antiabrasion property is a crucial challenge. After optimization, this coating could exhibit a conductivity of 42.46 S/m, which could maintain superhydrophobicity after 60 abrasion cycles.

Table 1: The experiment results of the superhydrophobicity with different contents of the filler.

Experiment	MWCNT (g)	EG (g)	Conductivity (S/m)	Antiabrasion (cycles)
1	0.10	0.00	1.96	600
2	0.15	0.03	4.26	300
3	0.20	0.04	8.53	80
4	0.30	0.05	42.46	60
5	0.35	0.06	138.14	5

Here, the soil was utilized as the model contaminant, and the glass slide was used as the substrate. As shown in Figure 6(a) and Movie S2, we first placed the superhydrophobic sample at a slope angle of ~15° and then spread a layer of soil onto the sample. In the next step, the water droplets were dribbled onto the sample. It can be found that the water droplets rolled down easily (Figures 6(b) and 6(c)). Once the water droplet contacted the soil particles, it would take the contaminant array due to the extremely low water adhesion. Finally, a completely clean sample was obtained (Figure 6(d)), suggesting the excellent self-cleaning property.

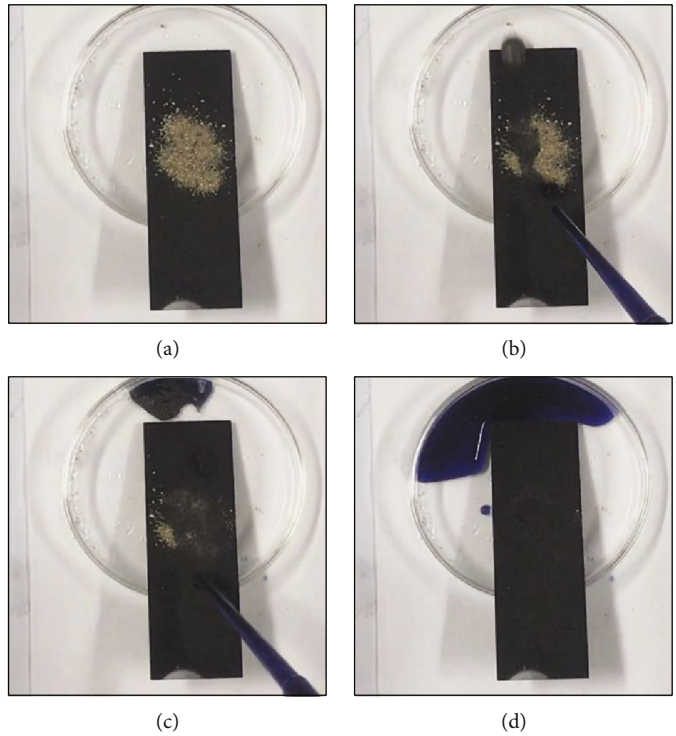

Figure 6: Self-cleaning process on the as-prepared superhydrophobic surface: (a) the surface contaminated by the soil powder; (b, c) the contaminated surface dropped with water droplets; (d) the contaminated surface after the water dropping process.

Moreover, this superhydrophobic coating exhibited excellent corrosion resistance [43–45]. The steel is universally utilized in our daily life due to their excellent mechanical strength, easy processing, and cost efficiency. Corrosion is regarded as the main failure mechanism for steel (especially for Q235 steel). In this research, we tried to improve the anticorrosive performance by means of superhydrophobic coating. The polarization curves were utilized to evaluate the corrosion resistance, as shown in Figure 7. Here, we employed the 3.5 wt% NaCl aqueous solutions as the electrolyte. Before the electrochemical test, we immersed the samples into the electrolyte for 3 h. Because the corrosion potential (E_{corr} vs. SCE) and the corrosion current density (i_{corr}) are two crucial for assessing the anticorrosive performance, we further deduced them from the polarization curves. The corrosion potentials for the bare Q235 steel, Q235 steel with epoxy coating, and superhydrophobic coating were calculated to be -0.198, -0.413, and -0.547 v, respectively. Furthermore, the corrosion current density for the bare Q235 steel, Q235 steel with epoxy coating, and superhydrophobic coating was calculated to be 2.41×10^{-5}, 6.24×10^{-6}, and 6.91×10^{-7} A/cm^2, respectively. Thus, the superhydrophobic coating could reduce the corrosion current density 35 folds compared with the bare sample and reduce 9 folds compared with the epoxy coating. We ascribed the outstanding corrosion resistance to superhydrophobicity. When the superhydrophobic coating was immersed in a corrosive solution, the micro/nanostructures of the coating tend to trap the air, which will serve as a cushion and hold back the electron transfer between Q235 steel substrate and the corrosive electrolyte [46, 47].

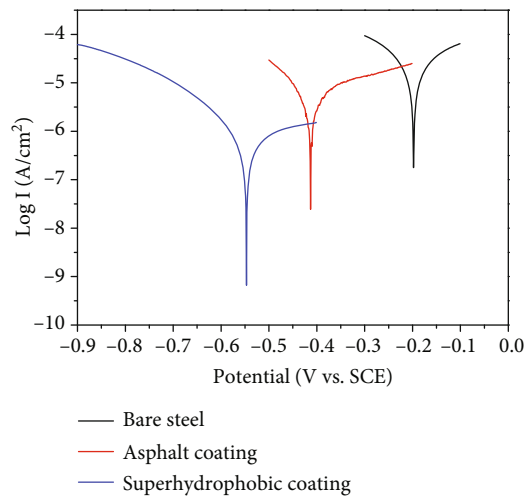

Figure 7: Tafel polarization curves of bare Q235 steel, epoxy coating, and superhydrophobic coating.

4. Conclusion

In summary, we reported a simple and cost-effective method to prepare superhydrophobic/conductive asphalt. The conductivity of the asphalt can be controlled by adding conductive filler. When the filler was dispersed uniformly in the asphalt matrix, the self-similar structure can be obtained. Moreover, the hierarchical structure could be constructed by adding nanoscale filler (carbon nanotube) and microscale filler (graphite powder and expanded graphite). Due to the

combination of self-similar and hierarchical structure, this superhydrophobic asphalt demonstrated mechanical robustness to the sandpaper abrasion. Moreover, this asphalt composite exhibited good conductivity, superior self-cleaning property, and excellent corrosion resistance.

Data Availability

The video data used to support the findings of this study are included within the supplementary information files.

Conflicts of Interest

The authors declare that they have no competing interests.

Acknowledgments

This work was supported by the State Grid Hebei Electric Power Research Institute (kj2019-063: the no-dig corrosion detection technology of the ground grid).

Supplementary Materials

The following are available online. Movie S1: the antiabrasion test. Movie S2: the self-cleaning test. *(Supplementary Materials)*

References

[1] G. Wu, E.-H. Choi, P. K. Chu, G. Dinescu, R. Jung, and Y. Zhao, "Recent applications of scanning microscopy in surface engineering," *Scanning*, vol. 2018, Article ID 7546310, 2 pages, 2018.

[2] P. Wang, T. Yao, B. Sun, T. Ci, X. Fan, and H. Han, "Fabrication of mechanically robust superhydrophobic steel surface with corrosion resistance property," *RSC Advances*, vol. 7, no. 63, pp. 39699–39703, 2017.

[3] Z. Wang, M. Wang, J. Jiang et al., "Atmospheric corrosion analysis and rust evolution research of Q235 carbon steel at different exposure stages in Chengdu atmospheric environment of China," *Scanning*, vol. 2020, Article ID 9591516, 8 pages, 2020.

[4] Y. Wang, G. Wu, and J. Sun, "Improved corrosion resistance of magnesium alloy in simulated concrete pore solution by hydrothermal treatment," *Scanning*, vol. 2020, article 4860256, pp. 1–7, 2020.

[5] Q. Zheng, K. Li, X. Yin et al., "Corrosion properties of 34CrMo4 steel modified by shot peening," *Scanning*, vol. 2017, Article ID 1928198, 8 pages, 2017.

[6] N. Wang, L. Tang, W. Tong, and D. Xiong, "Fabrication of robust and scalable superhydrophobic surfaces and investigation of their anti-icing properties," *Materials & Design*, vol. 156, pp. 320–328, 2018.

[7] N. Wang, L. Tang, Y. Cai, W. Tong, and D. Xiong, "Scalable superhydrophobic coating with controllable wettability and investigations of its drag reduction," *Colloids and Surfaces A: Physicochemical and Engineering*, vol. 555, pp. 290–295, 2018.

[8] X. Wang, M. Li, Y. Shen, Y. Yang, H. Feng, and J. Li, "Facile preparation of loess-coated membranes for multifunctional surfactant-stabilized oil-in-water emulsion separation," *Green Chemistry*, vol. 21, no. 11, pp. 3190–3199, 2019.

[9] X. Bai, Y. Shen, H. Tian, Y. Yang, H. Feng, and J. Li, "Facile fabrication of superhydrophobic wood slice for effective water-in-oil emulsion separation," *Separation and Purification Technology*, vol. 210, pp. 402–408, 2019.

[10] P. Wang, S. Wang, X. Zhang et al., "Rational construction of CoO/CoF_2 coating on burnt-pot inspired 2D CNs as the battery-like electrode for supercapacitors," *Journal of Alloys and Compounds*, vol. 819, article 153374, 2020.

[11] P. Wang, W. Wang, T. Ci, L. Li, and H. Han, "Pump-free oil droplet transfer by combining microfibre array and superoleophobic mesh," *Applied Surface Science*, vol. 455, pp. 980–986, 2018.

[12] G. Wei, Z. Wang, X. Zhao et al., "Pump-free oil droplet transfer by combining microfibre array and superoleophobic mesh," *Materials Research Express*, vol. 2, article 015501, 2015.

[13] R. Qiu, Z. Li, and Z. Wu, "Enhanced anti-icing and anti-corrosion properties of wear-resistant superhydrophobic surfaces based on Al alloys," *Materials Research Express*, vol. 6, no. 4, article 045059, 2019.

[14] N. Wang, D. Xiong, Y. Deng, Y. Shi, and K. Wang, "Mechanically robust superhydrophobic steel surface with anti-icing, UV-durability, and corrosion resistance properties," *ACS Applied Materials & Interfaces*, vol. 7, no. 11, pp. 6260–6272, 2015.

[15] Y. Cao, D. Zheng, X. Li et al., "Enhanced corrosion resistance of superhydrophobic layered double hydroxide films with long-term stability on Al substrate," *ACS Applied Materials & Interfaces*, vol. 10, no. 17, pp. 15150–15162, 2018.

[16] F. Zhang, H. Qian, L. Wang et al., "Superhydrophobic carbon nanotubes/epoxy nanocomposite coating by facile one-step spraying," *Surface and Coatings Technology*, vol. 341, pp. 15–23, 2018.

[17] M. Liu, Y. Hou, J. Li, L. Tie, Y. Peng, and Z. Guo, "Inorganic adhesives for robust, self-healing, superhydrophobic surfaces," *Journal of Materials Chemistry A*, vol. 5, no. 36, pp. 19297–19305, 2017.

[18] P. Wang, W. Wei, Z. Li, W. Duan, H. Han, and Q. Xie, "A superhydrophobic fluorinated PDMS composite as a wearable strain sensor with excellent mechanical robustness and liquid impalement resistance," *Journal of Materials Chemistry A*, vol. 8, no. 6, pp. 3509–3516, 2020.

[19] Y. Lu, S. Sathasivam, J. Song, C. R. Crick, C. J. Carmalt, and I. P. Parkin, "Repellent materials. Robust self-cleaning surfaces that function when exposed to either air or oil," *Science*, vol. 347, no. 6226, pp. 1132–1135, 2015.

[20] T. Verho, C. Bower, P. Andrew, S. Franssila, O. Ikkala, and R. H. A. Ras, "Mechanically durable superhydrophobic surfaces," *Advanced Materials*, vol. 23, no. 5, pp. 673–678, 2011.

[21] C. Peng, Z. Chen, and M. K. Tiwari, "All-organic superhydrophobic coatings with mechanochemical robustness and liquid impalement resistance," *Nature Materials*, vol. 17, no. 4, pp. 355–360, 2018.

[22] M. J. Nine, M. A. Cole, L. Johnson, D. N. H. Tran, and D. Losic, "Robust superhydrophobic graphene-based composite coatings with self-cleaning and corrosion barrier properties," *ACS Applied Materials & Interfaces*, vol. 7, no. 51, pp. 28482–28493, 2015.

[23] I. Hejazi, G. M. M. Sadeghi, S. H. Jafari et al., "Transforming an intrinsically hydrophilic polymer to a robust self-cleaning superhydrophobic coating via carbon nanotube surface embedding," *Materials & Design*, vol. 86, pp. 338–346, 2015.

[24] J. Gu, P. Xiao, J. Chen et al., "Robust preparation of superhydrophobic polymer/carbon nanotube hybrid membranes for highly effective removal of oils and separation of water-in-oil emulsions," *Journal of Materials Chemistry A*, vol. 2, no. 37, pp. 15268–15272, 2014.

[25] P. Wang, T. Yao, B. Sun et al., "A cost-effective method for preparing mechanically stable anti-corrosive superhydrophobic coating based on electrochemically exfoliated graphene," *Colloids and Surfaces A: Physicochemical and Engineering Aspects*, vol. 513, pp. 396–401, 2017.

[26] W. Li, Y. Wang, Y. Feng et al., "Fabrication of robust conductive and superhydrophobic coating based on carbon nanotubes," *Materials Research Express*, vol. 7, no. 5, article 055009, 2020.

[27] Y. Gao, L. Qu, B. He, K. Dai, Z. Fang, and R. Zhu, "Study on effectiveness of anti-icing and deicing performance of superhydrophobic asphalt concrete," *Construction and Building Materials*, vol. 191, pp. 270–280, 2018.

[28] P. Wang, M. Chen, H. Han, X. Fan, Q. Liu, and J. Wang, "Transparent and abrasion-resistant superhydrophobic coating with robust self-cleaning function in either air or oil," *Journal of Materials Chemistry A*, vol. 4, no. 20, pp. 7869–7874, 2016.

[29] N.-u.- H. Saddiqi and S. Seeger, "Chemically resistant, electric conductive, and superhydrophobic coatings," *Advanced Materials Interfaces*, vol. 6, no. 7, article 1900041, 2019.

[30] B. J. Basu, V. D. Kumar, and C. Anandan, "Surface studies on superhydrophobic and oleophobic polydimethylsiloxane-silica nanocomposite coating system," *Applied Surface Science*, vol. 261, pp. 807–814, 2012.

[31] N. Saleema, D. K. Sarkar, D. Gallant, R. W. Paynter, and X. G. Chen, "Chemical nature of superhydrophobic aluminum alloy surfaces produced via a one-step process using fluoroalkylsilane in a base medium," *ACS Applied Materials & Interfaces*, vol. 3, no. 12, pp. 4775–4781, 2011.

[32] H. Wang, J. Fang, T. Cheng et al., "One-step coating of fluoro-containing silica nanoparticles for universal generation of surface superhydrophobicity," *Chemical Communications*, vol. 877, no. 7, pp. 877–879, 2008.

[33] P. Wang, B. Sun, Y. Liang et al., "A stretchable and super-robust graphene superhydrophobic composite for electromechanical sensor application," *Journal of Materials Chemistry A*, vol. 6, no. 22, pp. 10404–10410, 2018.

[34] X. Zhang, L. Wang, and J. D. Sørensen, "REIF: a novel active-learning function toward adaptive Kriging surrogate models for structural reliability analysis," *Reliability Engineering & System Safety*, vol. 185, pp. 440–454, 2019.

[35] X. Zhang, L. Wang, and J. D. Sørensen, "AKOIS: an adaptive Kriging oriented importance sampling method for structural system reliability analysis," *Structural Safety*, vol. 82, p. 101876, 2020.

[36] J. Wang, L. Pan, Y. Bian, and Y. Lu, "Experimental investigation of the surface roughness of finish-machined high-volume-fraction SiCp/Al composites," *Arabian Journal for Science and Engineering*, vol. 45, no. 7, pp. 5399–5406, 2020.

[37] P. Wang, B. Sun, T. Yao et al., "A novel dissolution and resolidification method for preparing robust superhydrophobic polystyrene/silica composite," *Chemical Engineering Journal*, vol. 326, pp. 1066–1073, 2017.

[38] J. Song, D. Zhao, Z. Han et al., "Super-robust superhydrophobic concrete," *Journal of Materials Chemistry A*, vol. 5, no. 28, pp. 14542–14550, 2017.

[39] J. Song, F. Guan, W. Pan et al., "Droplet-based self-propelled miniboat," *Advanced Functional Materials*, vol. 30, no. 16, p. 1910778, 2020.

[40] J. Song, L. Huang, C. Zhao et al., "Robust superhydrophobic conical pillars from syringe needle shape to straight conical pillar shape for droplet pancake bouncing," *ACS Applied Materials & Interfaces*, vol. 11, no. 48, pp. 45345–45353, 2019.

[41] J. Song, Z. Liu, X. Wang et al., "High-efficiency bubble transportation in an aqueous environment on a serial wedge-shaped wettability pattern," *Journal of Materials Chemistry A*, vol. 7, no. 22, pp. 13567–13576, 2019.

[42] X. Tian, T. Verho, and R. H. A. Ras, "Moving superhydrophobic surfaces toward real-world applications," *Science*, vol. 352, no. 6282, pp. 142-143, 2016.

[43] X. Yin, Z. Wang, Y. Shen, P. Mu, G. Zhu, and J. Li, "Facile fabrication of superhydrophobic copper hydroxide coated mesh for effective separation of water-in-oil emulsions," *Separation and Purification Technology*, vol. 230, p. 115856, 2020.

[44] J. Li, R. Kang, X. Tang, H. She, Y. Yang, and F. Zha, "Superhydrophobic meshes that can repel hot water and strong corrosive liquids used for efficient gravity-driven oil/water separation," *Nanoscale*, vol. 8, no. 14, pp. 7638–7645, 2016.

[45] J. Li, L. Yan, X. Tang, H. Feng, D. Hu, and F. Zha, "Robust superhydrophobic fabric bag filled with polyurethane sponges used for vacuum-assisted continuous and ultrafast absorption and collection of oils from water," *Advanced Materials Interfaces*, vol. 3, no. 9, p. 1500770, 2016.

[46] P. C. Uzoma, F. Liu, L. Xu et al., "Superhydrophobicity, conductivity and anticorrosion of robust siloxane-acrylic coatings modified with graphene nanosheets," *Progress in Organic Coatings*, vol. 127, pp. 239–251, 2019.

[47] M. J. Kreder, J. Alvarenga, P. Kim, and J. Aizenberg, "Design of anti-icing surfaces: smooth, textured or slippery?," *Nature Reviews Materials*, vol. 1, no. 1, pp. 1–15, 2016.